

Impact of Integrating Renewable Energies into Distribution Networks on the Voltage Profile

S. S. ECH-CHARQAOUY ^{*,‡}, D. SAIFAOUY ^{*}, O. BENZOHRA ^{**}, A. LEBSIR ^{**}

^{*} Faculty of Sciences of Casablanca AC, Hassan II, University, Casablanca 20100, Morocco

^{**} Physics Laboratory, Faculty of Sciences of Casablanca AC, Hassan II University, Casablanca, Morocco

(echcharqaouy@gmail.com , ddsaifaoui@gmail.com , omar.benzohra@gmail.com , asmaalebsir4@gmail.com)

[‡] Corresponding Author; *Sidi Salah ECH CHARQAOUY*, 20100 Casablanca, Morocco, Tel: 00 212 661 31 93 55,

Fax: 00 212 522 34 05 44, echcharqaouy@gmail.com ,

Received : 27-12-2019 Accepted : 07-02-2020

Abstract-Voltage plane disruption represents one of the main problems encountered by Distribution Systems Operators due to the integration of dispersed generation. In this study, a novel approach to overcome this problem and study its impact has been adopted; a nodal topological model for a simple radial feeder is proposed. The development of mathematical model associated with a software application, provides an instantaneous voltage profile of the feeder, performs multi-criteria simulations, and improves this profile. Simulations show that the integration of dispersed productions, not exceeding 35% of the installed power (without action on the off-load tap-changer of the transformer) and 55% of this power (with an adjustment of the transformer output voltage at -5%), solves the problems of voltage drop at the end of the feeder. However, it has been observed that an integration rate greater than the above-mentioned rate causes overvoltage at certain injection points and degrades the voltage profile. the software calculates the adjustments to be made on the on-load tap-changer and the reactive and / or active powers to improve the voltage profile; In 99% of the cases the calculations converge and the profile is improved.

Keywords renewable energy; distribution network; integration; power quality.

1. Introduction

Morocco has potential in implementing renewable energies. The mean incoming solar rays vary from 4.7 to 5.6 kWh per day and per square meter in the country. Additionally, wind potential is promising, especially in northern and southern regions [1]. This is portrayed by the annual mean wind speed, which is between 9.5 and 11 m/s at 40 m above ground level from Essaouira, Tangier, and Tetouan and in the range 7.5 - 9.5 m/s at 40 m above ground level from Tarfaya, Taza, and Dakhla. Tangier, Tetouan and Taza are provinces in northern Morocco whereas Tarfaya, Dakhla are provinces in southern Morocco

Being conscious of this reality and the promising future of green energy resources, the Moroccan government has prioritized the development of renewable energies throughout

the Moroccan territory to increase its share up to 42% of the overall capacity by 2020 and to 52% by 2030. The government aims to enter a new phase, in the near future, by opening electricity produced by renewable energies to market competition [1]. Law 58-15 of 16 January 2016, following the publication of regulatory texts around 2020, will allow small and medium producers of renewable energies to integrate their productions into the Moroccan medium voltage (MV) and low voltage (LV) (50 to 1000 V) distribution grid. The French standard NFC 18510, with oligopolistic application in Morocco, determines the average voltage as HVA (high voltage level A), setting in the range 1000 - 50,000 V.

Considering the structure of the distribution grid and, in particular, the Moroccan distribution grid, new hardships need to be overcome and new problems have to be solved by

grid operators to ensure the safety of population and their estates in this new configuration, to maintain grid stability, avoid islanding and grid pollution, ensure an acceptable quality of the electric wave [2], and specifically maintain a regulatory voltage plane (contractual).

In this paper, a clear identification of the problem in the current context of the electric network LV operation of National Company of Electricity and Potable Water (ONEE) is proposed, meanwhile and try to establish a topographical node modelling (TNM). By applying some laws governing power flows and voltage drops, this MTN makes it possible to establish formulas for calculating the voltage profile at the different connection point of consumers and producers.

With the purpose of conducting multi-criteria simulations, a software application has been developed on MATLAB R2018a (MathWorks, Galway H91 P9KP Ireland) with numerous capabilities including the calculation of the voltage at every network point with or without the presence of renewable dispersed generations (RDGs), regardless the number or the location of RDG connections in this grid, besides corrective measures to enhance the voltage profile by acting on the transformer on-load tap changer for the reactive powers of the RDGs and/or their active powers.

2. Disruption of Voltage Plane

The voltage value in a radial network, where the flow evolves in one direction, is found to be reduced as a function of the distance between the source and the load (Figure 1-a and Figure 1-b). Therefore, one of the major concerns of the distributor consists on maintaining a voltage profile in the admissible ranges using LV feeders without resorting to further additional costs .

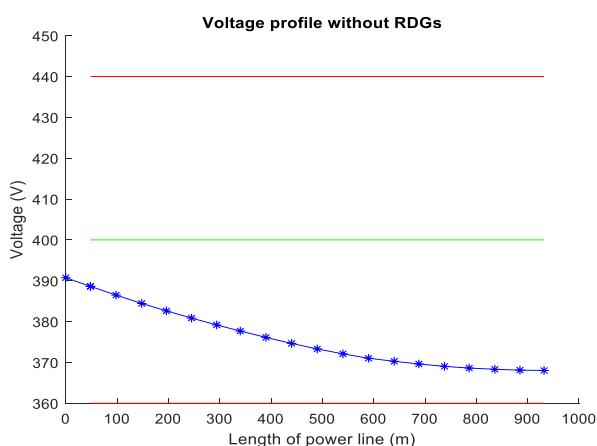


Figure 1-a : Voltage profile along a line (most loaded profile: summer, 20:00, Morocco local time);

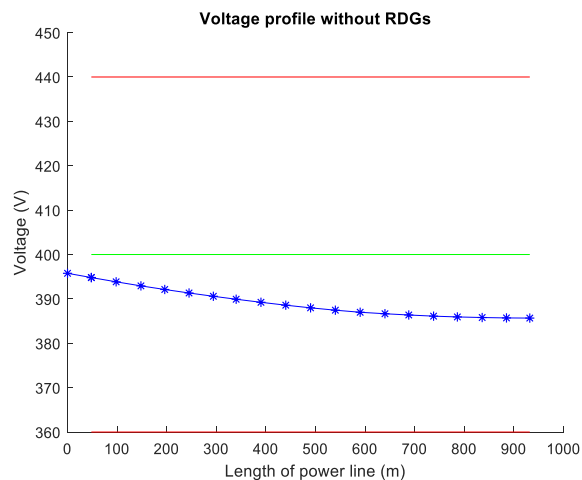


Figure 1-b : voltage profile along a line (least loaded profile: winter, 04:00, Morocco local time)

According to the existing standards and the subscription contracts of MV and LV customers, the distributors in Morocco must provide a voltage across terminal posts of $230\text{ V} \pm 10\%$ in single phase for LV customers and $400\text{ V} \pm 10\%$ in the three phases between phases. Similarly, for medium voltage (MV), customer subscription contracts compel ONEE to provide $22\text{ KV} \pm 10\%$ voltage at their connection points

The structure of 90% of the Moroccan network that was developed under the National Rural Electrification Program (PERG) is illustrated in Figure 2

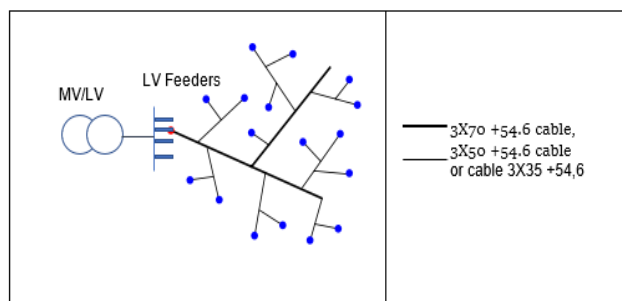


Figure 2. General structure of the low voltage (LV) National Rural Electrification Program (PERG) Moroccan network. MV denotes medium voltage

The voltage setting currently adopted by ONEE is seasonal, performing a power-off operation at the switcher HVA/LV through three possibilities, i.e. -5% , 0% , and 5% .

This setting is designed mainly to avoid over-voltage—surpassing the normative threshold—across the terminal connections of the first customer in the case of the least loaded profile (minimum load), as well as to minimize the voltage drops lower than the normative threshold across the terminal connections of the last customer at the end of the feeder [3].

In the case of RDG production injection, this method has been found to be inefficient with certain limitations. Injecting

relatively large power into the grid affects the direction of the energy current flow and generates over-voltages at the point of injection, thereby disrupting the voltage profile. The impact of integrating production into a voltage plane depends on the power produced, the power called by the feeder, and the injection location.

It is important to highlight that voltage drops appear during the maximum load without a producer whereas over-voltages appear at the time of injecting a large production into the network during minimum load.

For the integration of a dispersed electrical generation production into the network, two cases are possible depending on the power called by the feeder, the power produced, and the connection conditions. The producer may maintain a voltage plane or even improve it, or may disturb it by generating an over-voltage (especially with minimum load).

Figures 3-a and 3- b depict the presence of over-voltages at the last nodes of the feeder between 08:00 and 17:00 Morocco local time.

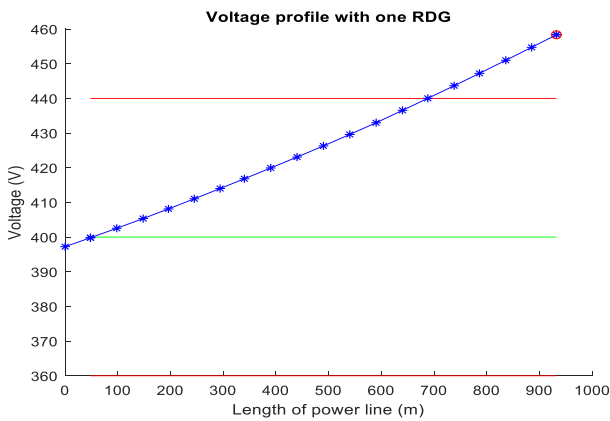


Figure 3-a: Voltage profile with the integration of a single renewable dispersed generation (RDG) at the end of the feeder;

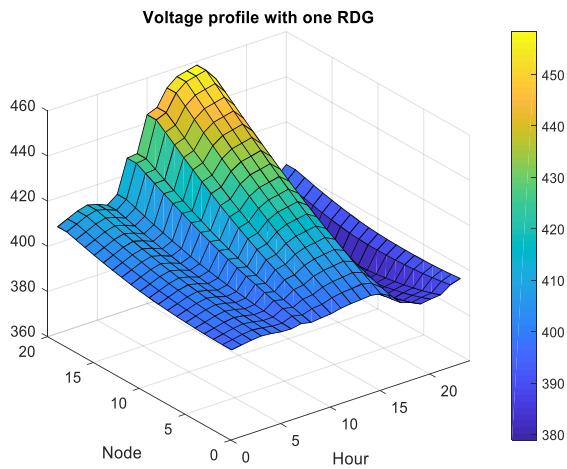


Figure 3-b: voltage profile along the feeder during the day

3. Topological Node Modeling

To further investigate this problem, it was necessary to determine the voltage profile of the studied line then calculate the voltage value at each of its nodes. For this purpose, the adopted solution is to set up a topological node model of the feeder, while considering clients and RDG producers' connection points, as shown in Figure 4.

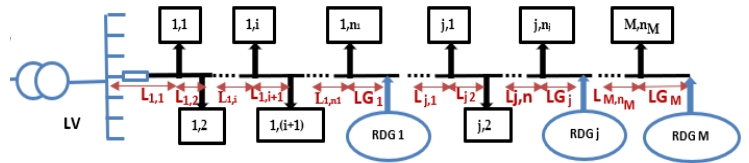


Figure 4. Simplified line diagram with different nodes: connection points of customers and RDGs.

Where n_1 represents the number of clients connected upstream the connection point of RDG $n^\circ 1$, n_j the number of clients connected between the connection points of RDG $n^\circ(j - 1)$ and RDG $n^\circ j$, n_{M-1} the number of clients connected between the connection points of RDG $n^\circ(M-2)$ and RDG $n^\circ(M-1)$, n_M the number of clients connected between the connection points of RDG $n^\circ(M-1)$ and the network end (RDG fictive M of zero production), N the total number of clients then ($N = \sum_{j=1}^M n_j$), $(M-1)$ the number of real RDGs, N_{ji} the ranked nodes (i) on the landing between ranked RDGs ($(j - 1)$ and j), G_j the ranked RDG (j), L_{ji} the Length of the line segment between ranked node ($i - 1$) and ranked node (i) on the landing between the two RDG ($(j - 1)$ and (j)), LG_j the length of the line segment between ranked node (n_j): last node of the landing $[(j - 1), j]$ and producer (G_j) ($LG_M = 0$ /ranked RDG M is fictive), P_{ji} the active power value at node (j, i) in (W), PG_j the active power value of RDG number j in (W), Q_{ji} the reactive power value of RDG number j in VAR (volt-ampere reactive), QG_j the reactive power value of RDG number j in (VAR)

To determine the voltage profile, it is important to calculate the voltage drops at different nodes of the feeder, following the topology illustrated in Figure 4.

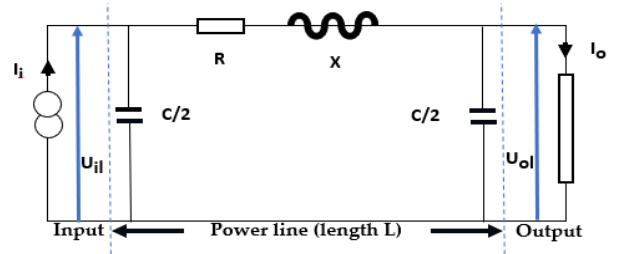


Figure 5-a : Modeling of the power line;

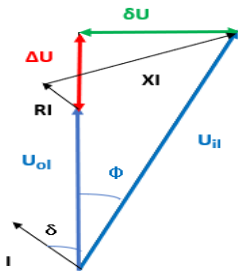


Figure 5-b : Fresnel construction for calculating voltage drops

From Figure 5b, it can be concluded that voltage drops proceed according to the following equation:

$$\Delta U = U_{il} - U_{o1} = R I \cos\phi + X I \sin\phi. \tag{1}$$

where ΔU represents the change in voltage, U_{il} the voltage at the entrance of the line in (V), U_{o1} the voltage at the output of the line in (V), R the line resistance in (Ω), X the line reactance in (Ω), ϕ the phase angle and I the current value in (A).

Considering the resistance (r) and reactance (x) per unit length along the line, the voltage drop ΔU is written as $\Delta U = r L I \cos\phi + x L I \sin\phi$, where L is the length of the line, ϕ the phase angle, P the active power, Q the reactive power and U_{il} the value of voltage at the input of the line. Hence:

$$\Delta U = \frac{L}{u_{il}} (rP + xQ). \tag{2}$$

By applying this formula to different nodes along the feeder, the following general equations can be obtained:
 1)

$$\Delta U_{fk} = \frac{L_{fk}}{(U_{f(k-1)})} \left(r \left[\sum_{i=k}^{n_f} P_{fi} + \sum_{j=f+1}^M \sum_{i=1}^{n_j} P_{ji} - \sum_{j=f}^M P_{Gj} \right] + x \left[\sum_{i=k}^{n_f} Q_{fi} + \sum_{j=f+1}^M \sum_{i=1}^{n_j} Q_{ji} - \sum_{j=f}^M Q_{Gj} \right] \right) \tag{3}$$

$$\Delta U_{Gf} = \frac{L_f}{(U_{fn_f})} \left(r \left[\sum_{j=f+1}^M \sum_{i=1}^{n_j} P_{ji} - \sum_{j=f}^M P_{Gj} \right] + x \left[\sum_{j=f+1}^M \sum_{i=1}^{n_j} Q_{ji} - \sum_{j=f}^M Q_{Gj} \right] \right) \tag{4}$$

$$S\Delta U_{fk} = \left(\sum_{j=1}^{f-1} \sum_{i=1}^{n_j} \Delta U_{ji} + \sum_{i=1}^k U_{fi} + \sum_{j=1}^{f-1} \Delta U_{Gj} \right) \tag{5}$$

$$S\Delta U_{Gf} = (S\Delta U_{fn_f} + \Delta U_{Gf}) \tag{6}$$

$$U_{fk} = (U_s - S\Delta U_{fk}) \tag{7}$$

$$U_{Gf} = (U_s - S\Delta U_{Gf}). \tag{8}$$

Where U_{ji} represents the value of the voltage at the node (j, i) , U_{Gj} the value of the voltage at the connection point of the RDG no. j , ΔU_{ji} the value of the voltage drops between the node $N(j, i-1)$ and the node $N(j, i)$, ΔU_{Gj} the value of the voltage drops between the node $N(j, n_j)$ and the connection point of RDG no. j , $S\Delta U_{ji}$ the Sum of the voltage drops between the node $N(j, 1)$ and the node $N(j, i)$, $S\Delta U_{Gj}$ the Sum of the voltage drops between the node $N(j, 1)$ and the connection point of the RDG no. j , r the linear resistance in (Ω/m), x the linear reactance (in Ω/m).

To consider the variation in power required by consumers during the day, the studied daily load profile curve has been examined. The general appearance of this curve for the Moroccan network is shown in Figure 6. The RDGs connected to the studied grid are of photovoltaic (PV) type, and their production varies depending on many parameters (irradiation, temperature, moisture content, and other spatial and

geometrical parameters). On a clear day, the general appearance of the production is depicted in Figure 7.

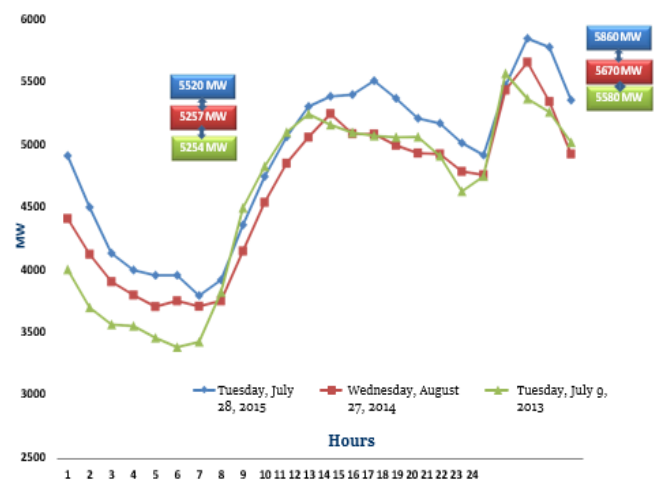


Figure 6. Trend in the daily load curve.

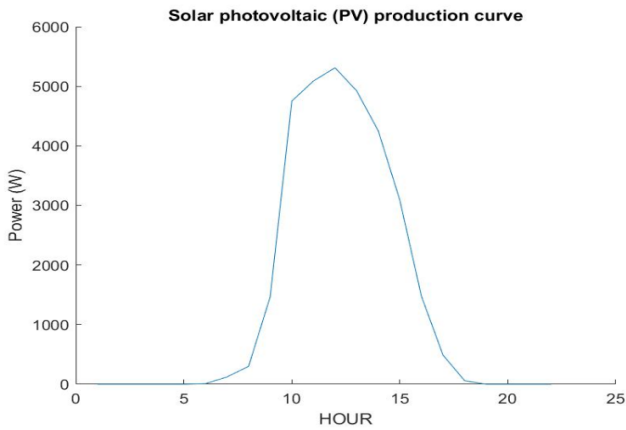


Figure 7. Solar photovoltaic (PV) production curve during a single day in June 2019 in Rabat, Morocco.

We consider that the level of active and reactive powers injected by the production plants is sufficiently controlled [4]

Some hypotheses are considered to simplify the approach, namely: (i) the power installed at the station is supposedly inferior to the MV starting power that feeds the station to avoid generating MV voltage drops at its connection point; (ii) the injected maximum power should never exceed the

transformer load to avoid an energy flow toward the MV network; (iii) in the absence of data on energy storage operated by producers, an average rate of 30% was assumed.

The voltage at the output of the transformer in charge is given by:

$$U_s = U_0 - \frac{R_{tr} \times P - X_{tr} \times Q}{U_0}, \tag{9}$$

where U_0 represents the vacuum voltage transformer; R_{tr} and X_{tr} the resistance and transformer reactance, respectively; and P and Q the active power and the reactive power called from the powered network from this transformer, respectively.

Simulations were performed in VOPROCA_DG (voltage profile calculation with dispersed generations) developed by our team in MATLAB R2018a (MathWorks, Galway H91 P9KP Ireland). This is an application designed to provide the voltage profile of each node of an electrical line each hour, regardless the number of producers and their placements. It allows the tracing of a three-dimensional (3D) curve that expresses voltage versus node placements and time.

The simplified algorithm of this application is provided in Figure 8.

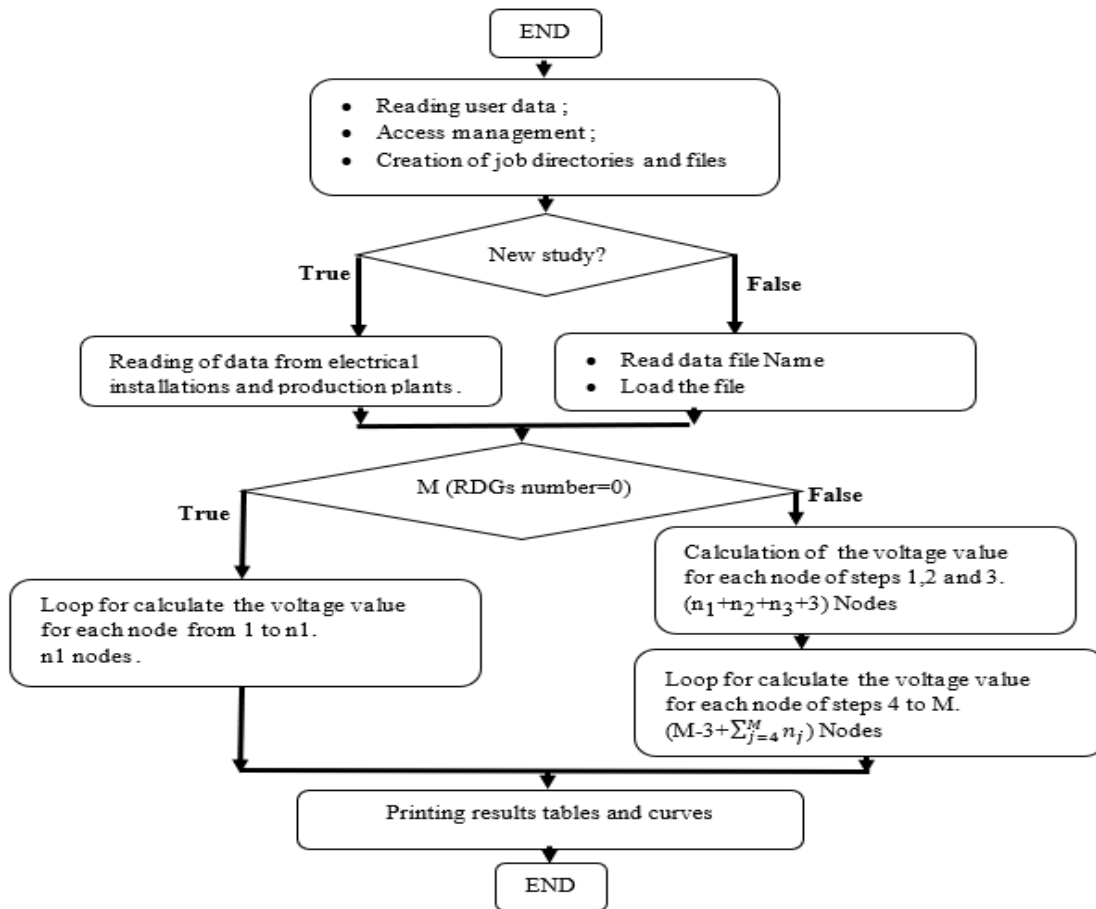


Figure 8. Simplified algorithm, VOPROCA_DG (voltage profile calculation with dispersed generations).

4. Simulations and Discussion

Simulations were performed on an LV line derived from the MV/LV substation of Al Fokra village in Ben Slimane city, Morocco. A 22 KV/400 V transformer of 250 KVA, feeding three LV lines, equips the substation. The line affected by energy injections is 932 m in length and feeds 19 LV clients.

The injections were established based on the PV module station with a power of 6700 W, which has a 41 m² surface of solar panels, covering a land surface area of 35 m². It is composed of 24 panels (VOLTEC SOLAR, TARKA 60, VOLTEC SOLAR, DINSHEIM SUR BRUCHE, France) with a unitary power of 282 Wp (Watt peak) each, and an inverter (5 kW; SMA Sunny TRIPOWER 5000 TL, SMA Solar Technology AG Sonnenallee 1 34266 Niestetal Germany).

The physical and geometric data of the electrical components, installations and works used in the simulations are summarized in tables 1 and 2

Table n°1 : the main input data and physical properties used for the simulation

22 KV / 400 V substation (250 KVA)	R= 8.32E-03 Ω X= 2.42E-02 Ω
Twisted aluminum cable 3*70 mm ² +54.6 mm ²	linear resistance r= 0.443 10 ⁻³ Ω/m
	Linear reactance x=8 10 ⁻⁵ Ω/m
φ _c : Consumption phase angle	Cos φ _c =0,8
	tg φ _c =0,75
φ _p : Production phase angle	Cos φ _p =0,9
	tg φ _p =0,48

Table n°2 : Physical data of the nodes

Node	Distance between nodes (m)	Distance between node and transformer (m)	Active power (kW)	Reactive power (kW)
N(1,1)	48	48	1,80	1,35
N(1,2)	50	98	2,25	1,69
N(1,3)	50	148	3,45	2,59
N(1,4)	48	196	2,25	1,69
N(1,5)	49	245	2,25	1,69
RDG(1)	0	245	20,00	9,6
N(2,1)	49	294	1,80	1,35
N(2,2)	46	340	1,80	1,35
N(2,3)	50	390	1,80	1,35
N(2,4)	50	440	2,70	2,03
N(2,5)	50	490	3,30	2,48
RDG(2)	0	490	15,00	7,2
N(3,1)	50	540	2,93	2,19
N(3,2)	50	590	6,60	4,95
N(3,3)	50	640	1,80	1,35
N(3,4)	48	688	1,80	1,35
RDG(3)	0	688	10,00	4,8
N(4,1)	50	738	3,38	2,53
N(4,2)	48	786	2,70	2,03
N(4,3)	50	836	1,80	1,35
N(4,4)	49	885	2,70	2,03
RDG(4)	0	885	20,00	9,6
N(1,5)	47	932	1,80	1,35
GED(5) fictional	0	932	0,00	0
TOTAL	932	932	48,90	36,68
Production / installed customer power	102%			
Production / power installed at the substation	25%			

The objective of these simulations was to better define the conditions of disturbances and to propose solutions. The voltage profile was defined for a line operating without RDG, with an injection of one RDG at the end of the line, one in the middle of the line, and four distributed along the line more or less regularly.

Before the integration of the RDGs, the feeder experiences a slight voltage drops at the connection point of the last customer. This voltage drop has been recorded when the load is at the maximum at around 20:00, as shown in Figure 9-a. This problem is then solved by changing the transformer tap changer from 0% to 5%. The open circuit voltage of the transformer increases from 400 to 420 V and the voltage drop disappears, as shown in Figure 9-b. The voltage for the last customer increases from 354 to 376 V.

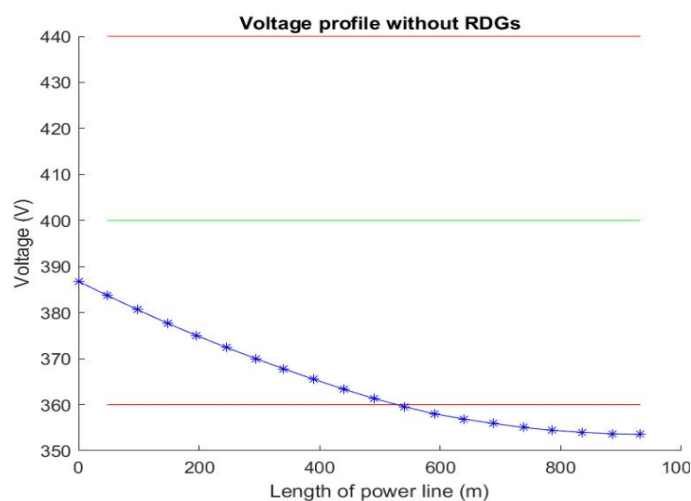


Figure 9-a. Voltage profile along the power line (most loaded profile: summer, 08:00 pm local time) with setting the voltage tap changer to 0% ($U = 400$ V)

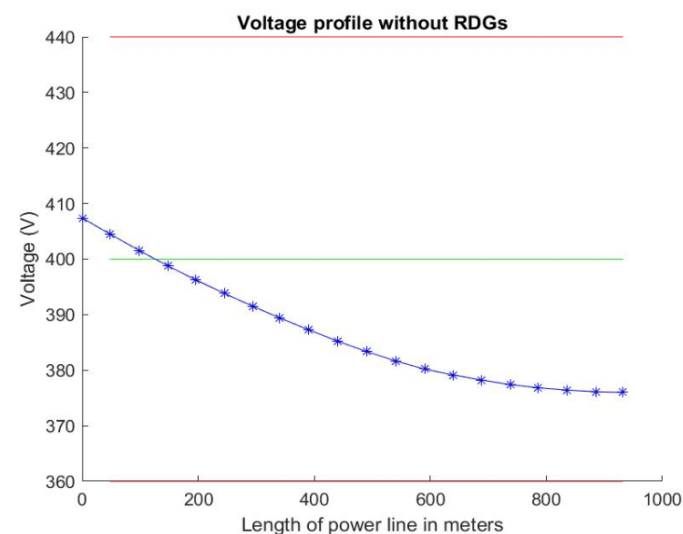


Figure 9-b Voltage profile along the power line (most loaded profile: summer, 08:00 pm local time) with setting the voltage tap changer to 5% ($U = 420$ V).

The injection of RDG at the end of the line, with a maximum production power of 15 kW being 31% of the line load and 8% of power installed at the MV/LV substation, significantly improved the profile voltage along the line. This enhancement has been observed for all hours of the day, without resorting to any adjustment, as shown in Figures 10-a and 10-b.

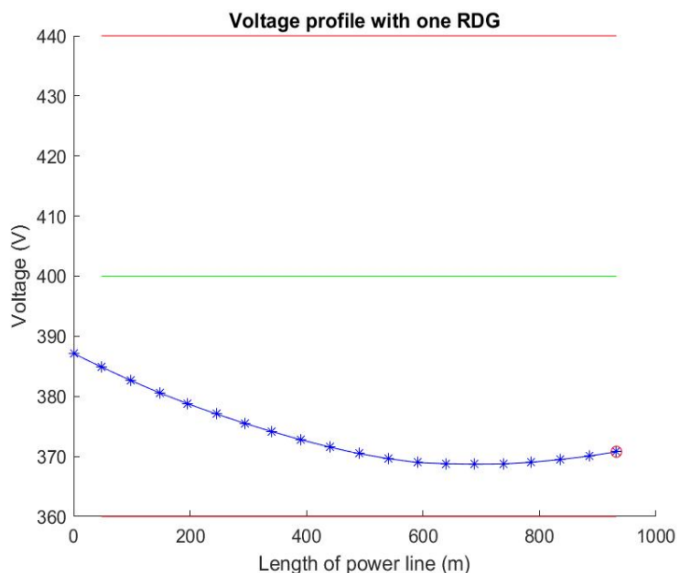


Figure 10-a Voltage profile along the power line (most loaded profile: summer, 08:00 pm local time);

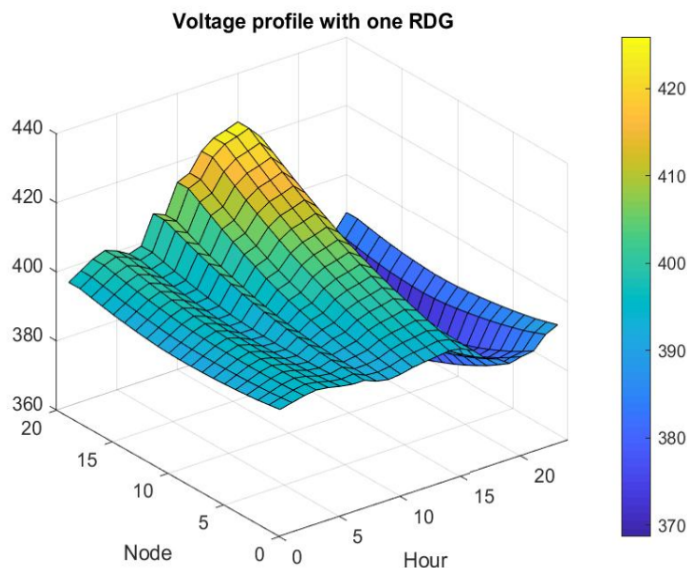


Figure 10-b Three-dimensional (3D) voltage profile along the power line over 24 h.

However, the injection of RDG with the limit power reaching the power required by the line (48.9 kW), whether at the end or in the middle of the line, remains positive, and the voltage profile notably improves.

Figures 11-a and 11-b taken during RDG injection on the middle of the line, depict the voltage profile at 15:00, the hour of maximum production, and at 20:00 representing the peak hour of consumption. These two figures show that the voltage varies between a maximum value of 410 V recorded at 15:00 at the RDG connection node N (1,10), and a minimum value of 364 V recorded at 20:00 at the last node of line N (2,9), with a fictitious RDG of zero power where the voltage record the greatest drop. Figure 11-c depicts a 3D profile for a 24 h period, illustrating this finding. Considering their form, these curves are named “saddle curves”.

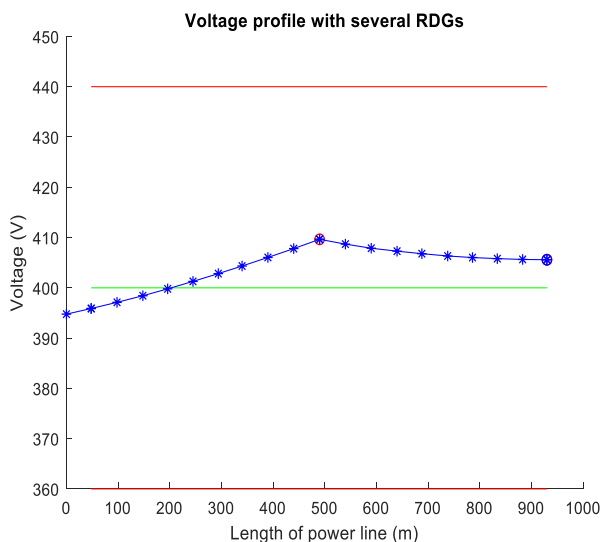


Figure 11-a. Voltage profile along the power line during summer at 03:00 pm

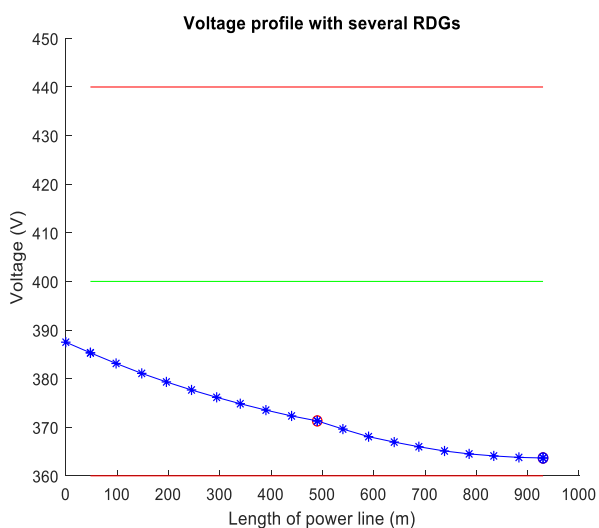


Figure 11-b Voltage profile along the power line when most loaded during summer at 08:00 pm

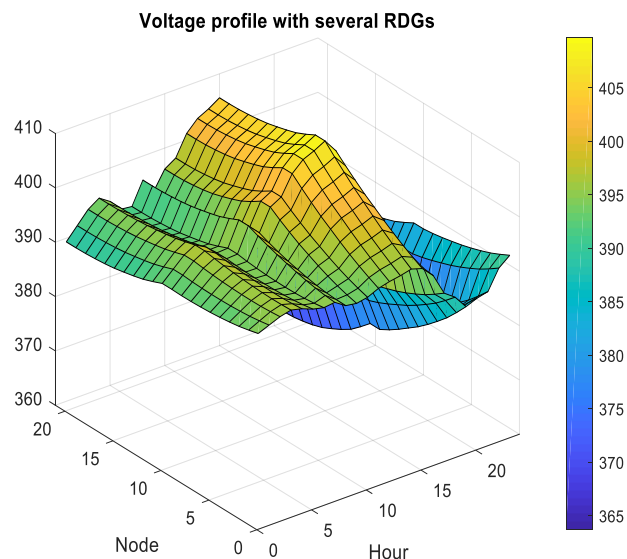


Figure 11-c 3D voltage profile along the power line for 24 h.

Similar to the above figures, Figures 12-a and 12- b created during RDG injection at the end of the line, depict the voltage profile at 15:00 corresponding to the hour of maximum production, and at 20:00 representing the peak hour of consumption. In this case, it can be observed that the voltage varies between a maximum value of 426 V recorded at 15:00 at the RDG connection node, and a minimum of 369 V recorded at 20:00 at the node N (1,14), where the voltage drops is at its maximum. The saddle curve in Figure 12-c, which depicts a 3D profile for a 24 h period, illustrates this finding. the injection of an RDG whose maximum power exceeds 48.9 KW generates over-voltages on the feeder.

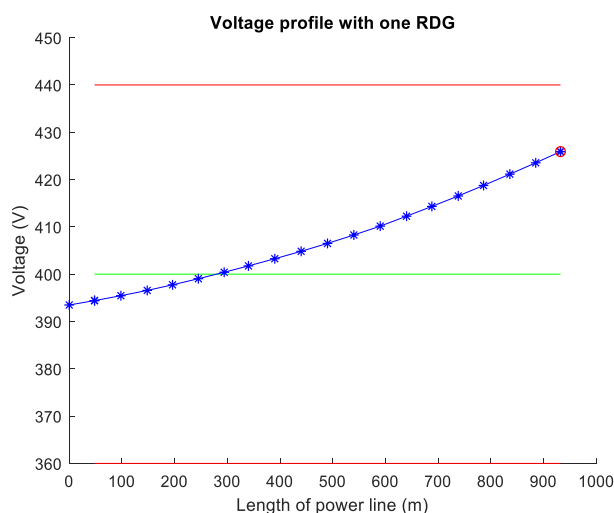


Figure 12-a Voltage profile along the power line during the most loaded profile (One RDG of PG=48,9 KW integrated at de bottom's feeder in summer at 03:00 pm);

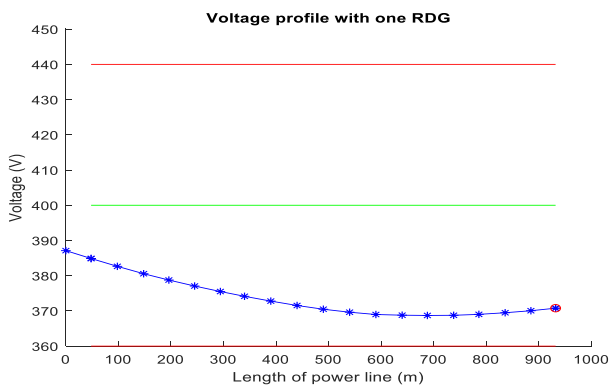


Figure 12-b. Voltage profile along the power line during the most loaded profile: (One RDG of PG=48,9 KW integrated at de bottom's feeder in summer at 08:00 pm);

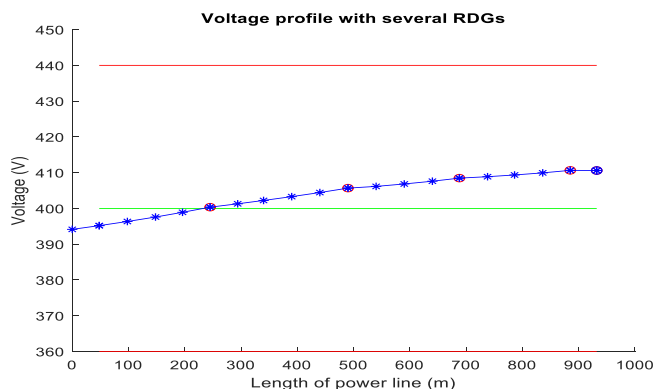


Figure 13-b. Voltage profile along the power line at 1:00 pm (Four RDGs with 48.9 kW of production)

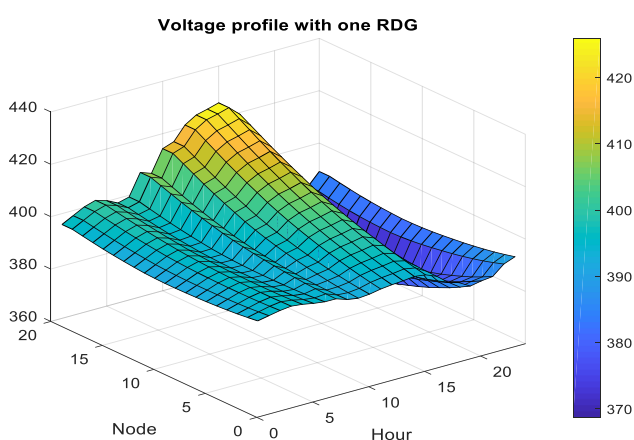


Figure 12-c : 3D profile for a 24 h period in summer (One RDG of PG=48,9 KW integrated at de bottom's feeder)

The injection of four RDGs, in which the sum of produced powers is less than or equal to the power required by the line (48.9 kW), at regular positions along the line, allowed to straighten the instantaneous voltage profile, as illustrated in Figures 13-a and 13-b. Similarly, in Figure 13-c, the saddle curve, depicting a 3D profile for a 24 h period, shows that the voltage profile lies between 375 and 415 V.

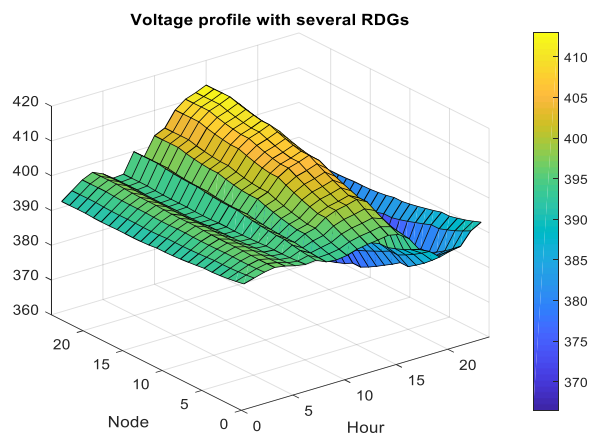


Figure 13-c 3D voltage profile over 24 h.

RDG's injection at the end of the line, with maximum production of 75 KW (37.5% of the installed power of the transformer station) has generated an overvoltage of 15 % at 3 p.m. (hour where the RDG production is at its maximum), giving 458V at the RDG connection (see Figure 14-a). Over voltages are noted during all hours of the day, while the RDG's production remains stable as illustrated on the saddle curves without object of Figure 14.b.

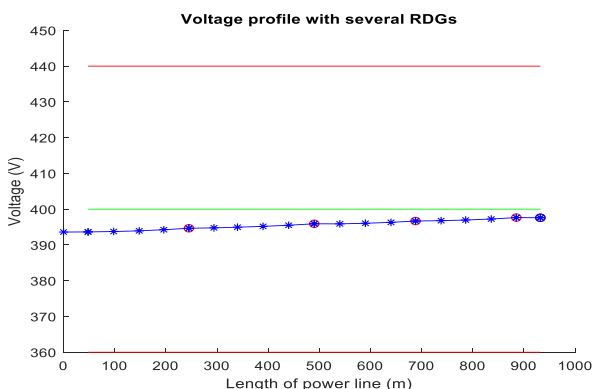


Figure 13-a. Voltage profile along the power line at 09:00 am . (Four RDGs with 48.9 kW of production)

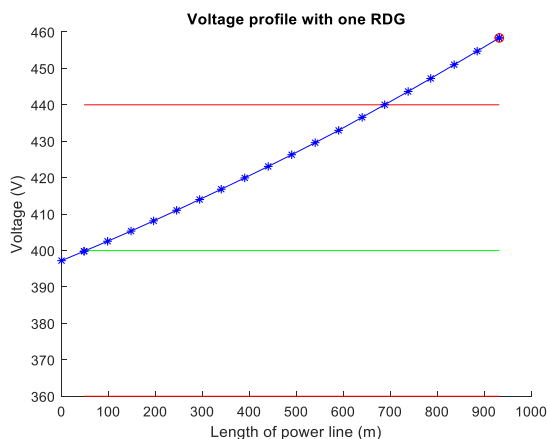


Figure 14-a. Voltage profile along the power line at 03:00 p.m. (One RDG at the bottom's feeder)

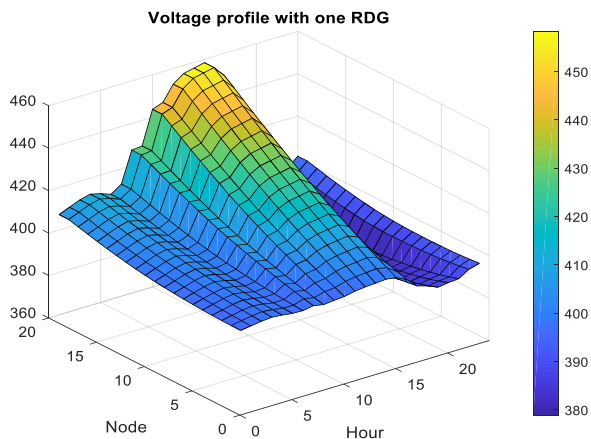


Figure 14-b. 3D voltage profile over 24 h (One RDG integrated at the bottom's feeder).

Overvoltage are also detected during the injection of four RDGs (30, 30, 20 and 30 KW) representing 55% of the power of the transformer.

The maximum overvoltage has been recorded at the connection point of the last RDG with a voltage of 454 V and a voltage drop of 13.6%, as illustrated by the curves in Figures 15-a and 15-b.

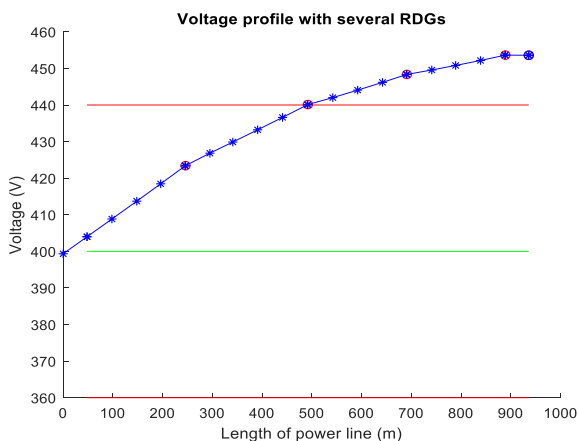


Figure 15-a. Voltage profile along the power line at 03:00 p.m. (Four RDGs)

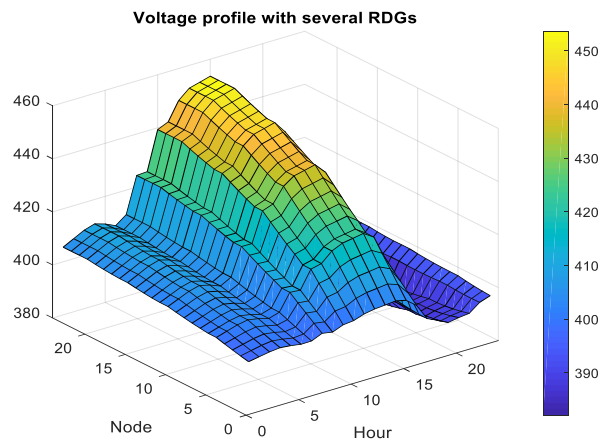


Figure 15-b 3D voltage profile over 24 h. (Four RDGs integrated into the feeder).

It is not easy to make a conclusion regarding the network reception capacity based on the results of a limited number of simulations. Indeed, for the last simulation the results completely change by adjusting the transformer off-load tap changer. It is enough to lower the open circuit voltage of 5% and the overvoltage disappears. It should be noted that no voltage drop was recorded. The most loaded profile at 08:00 pm local time records the lowest voltage (361 V) at node N (4,2). So, it borders on a voltage drop. As for the highest voltage(436 V), it is recorded at 03:00 pm at node N (5,1).

This simulation is the most informative on the reception capacity. Effect the maximum tension and the minimum tension on the 24 hours reach their extreme values (see Figures 16-a et 16-b)

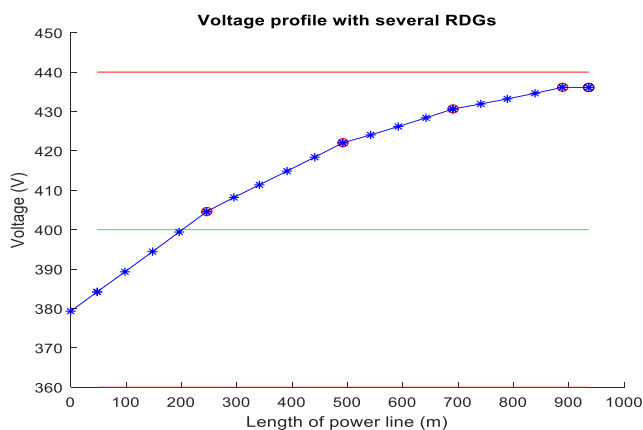


Figure 16-a. Voltage profile along the power line at 03:00 p.m. and $U_0=400V - 5\%$

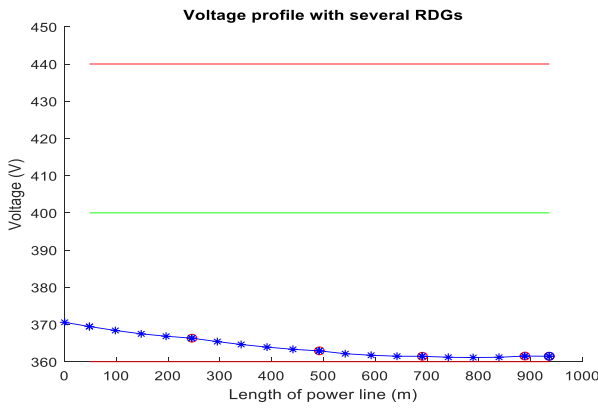


Figure 16-b. Voltage profile along the power line at 08:00 p.m. and $U_0=400V - 5\%$

4.1 Application of the Method to Solve the Disruption Problem of Voltage Planes

The literature reveals that several methods to improve the voltage profile and rebalance the alternating current (ac) grid voltage asymmetries, have been studied, we cite in other the network reconfiguration, the action on the reactive energy circulating in the network [5][6]. In our approach we tried to find the right mix between several methods

When RDG integration exceeds a given threshold, the voltage plane is disrupted. An analysis of the phenomenon, based on the mentioned formulas, reveals that voltage variation depends only on the transformer open circuit voltage [3] and upon active and reactive powers of RDGs, while assuming that powers consumed by clients are constant. The following equations are proposed:

$$B_{fk} = \frac{L_{fk}}{(U_f^{(k-1)})} \times r \left[\sum_{i=f}^{n_f} P_{fi} + \sum_{j=f+1}^M \sum_{i=1}^{n_j} P_{ji} \right] \quad (10)$$

$$D_{fk} = \frac{L_{fk}}{(U_f^{(k-1)})} \left(x \left[\sum_{i=f}^{n_f} Q_{fi} + \sum_{j=f+1}^M \sum_{i=1}^{n_j} Q_{ji} \right] \right) \quad (11)$$

$$A_{fk} = \frac{L_{fk}}{(U_f^{(k-1)})} \times r \quad (12); \quad C_{fk} = \frac{L_{fk}}{(U_f^{(k-1)})} \times x \quad (13)$$

$$\Delta U_{fk} = B_{fk} - A_{fk} * \sum_{j=f}^M P_{G_j} + D_{fk} - C_{fk} * \sum_{j=f}^M Q_{G_j} \quad (14)$$

Hence, by controlling the active powers PG_i and reactive powers QG_i of RDGs, it is possible to control the voltage variation (either increase or decrease).

The method is based on vector calculation $(OV)_i$ and $(VD)_i$, representing vectors of over-voltages and voltage drops at the nodes of the line, respectively:

$$(OV)_i = (U_{node} - 1.1U_0)_i \quad (15); \quad (VD)_i = (0.9U_0 - U_{node})_i \quad (16)$$

Where U_0 is the vacuum rated voltage of the transformer.

In the case of over-voltage, the first step consists on adjusting the transformer on-load tap changer and launching

an iteration calculation of the voltage profile. This operation is repeated as long as this profile remains damaged. If the action on the voltage adjuster under load is insufficient to improve the voltage profile, the power of QG_i is reduced for all over-voltage producers ($\alpha_i * \Delta Q$), where ΔQ is the capacitor's battery step with α_i numbers of batteries and α_i numbers of steps to implement. The parameter α_i is calculated in proportion to the value of the over-voltage. Profile calculation iterations are carried out and repeated until a suitable profile is obtained. If this step is also insufficient, active powers similarly is then treated. The same process is adopted for voltage drops, except that instead of reducing QG_i values, they are increased. The simplified algorithm of the adopted method is presented in Figure 16.

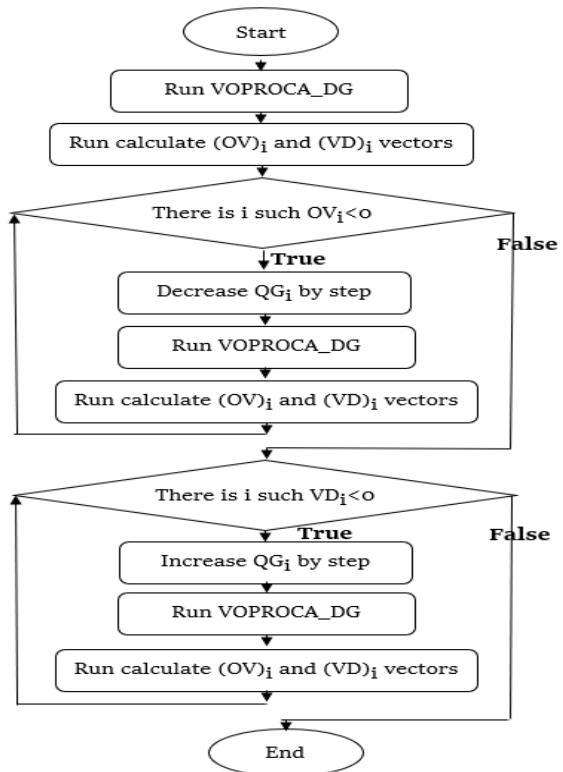


Figure 16. Simplified algorithm/enhancement voltage profile subroutine.

where $(OV)_i$ and $(VD)_i$ represent vectors of over-voltages and voltage drops at the nodes of the line, respectively. OV_i is the rank i term in the vector $(OV)_i$ and VD_i is the rank i term in the vector $(VD)_i$.

This application is part of a smart grid project upstream and downstream of the client–producer meter.

Our software provides command and control of electrical installations, namely load regulators for transformers, smart meters[7](bidirectional and communicating) and production plants.[8], [9].

the smart grid downstream of the meter represents a compatible solution with the studies developed in the literature to optimize the use of hybrid power plants [10].

5. Conclusion

In this study, a newly developed approach based on nodal modeling besides composing formulas that provide the voltage at each node of a line regardless the number of clients and producers, is presented, thereby allowing to perform multi-criteria simulations.

The obtained results demonstrate that the integration of dispersed productions, not exceeding 35% of the installed power at the transformer HVA/LV (without action on the off-load tap-changer of the transformer) and 55% of this power (with an adjustment of the transformer output voltage at -5%), solves the problems of voltage drop at the end of the feeder. However, it has been observed that an integration rate greater than the above-mentioned rate causes overvoltage at certain injection points and degrades the voltage profile at the minimum value of the Rp ratio:

$$R_p = \frac{\text{Demand Power}}{\text{Output Power of RDGs}} \quad (17)$$

The simulations indicate that an improvement in the voltage profile is possible in most cases by adjusting the transformer on-load tap changer for reactive power and active powers. These actions must obey the following priority pattern:

1. Act first on the transformer on-load tap changer;
2. If this operation proves insufficient, launch iterations to determine actions to be taken on the reactive powers of RDGs; and
3. If this second action proves to be insufficient, start iterations to determine actions on active powers of RDGs.

This multi-purpose project aims to provide one of the most important elements of the real-time network voltage regulation platform. It is an essential aspect in an integral smart grid solution.

In fact, our software provides command and control of electrical installations, namely load regulators for transformers, smart meters (bidirectional and communicating) and production plants.

Limits of the solution can be observed during significant variations in the HVA voltage exceeding the tolerated thresholds (+ or - 10%) for long periods.

This study provides for an improvement of the software to manage an entire network from an HVA / LV station.

References

- [1] M. Enzili. L'énergie éolienne au Maroc In Proceedings of the Potential and Projects, 6th Conference Maroc—Allemande sur L'énergie Eolienne, Casablanca, Morocco, 15 November 2011.
- [2] Shobole, Abdulfetah & Baysal, Mustafa & Wadi, Mohammed & Tur, Mehmet Rıda. (2017). Effects of distributed generations' integration to the distribution networks case study of solar power plant. *International Journal of Renewable Energy Research*. 7. 954-964. Vol 7, No 2 (2017) pp 954-964
- [3] Xu, T.; Taylor, P.C. Voltage Control Techniques for Electrical Distribution Networks Including Distributed Generation, School of Engineering, University of Durham, UK. In Proceedings of the 17th World Congress of the International Federation of Automatic Control, Seoul, Korea, 6–11 July 2008, pp 11967-11971
- [4] Turitsyn, Konstantin & Sulc, Petr & Backhaus, Scott & Chertkov, Michael. (2010). Local Control of Reactive Power by Distributed Photovoltaic Generators. *Smart Grid Communications (SmartGridComm)*, 2010 First IEEE International Conference. pp 79 - 84..
- [5] John Prousalidis, George Antonopoulos, Panagiotis Mouzakis & Elias Sofras (2015) On resolving reactive power problems in ship electrical energy systems, *Journal of Marine Engineering & Technology*, 14:3, pp 124-136
- [6] A. Lachichi, "Modular multilevel converters with integrated batteries energy storage," *2014 International Conference on Renewable Energy Research and Application (ICRERA)*, Milwaukee, WI, 2014, pp. 828-832.
- [7] S. N. Saxena, (December, 2019). Smart Distribution Grid – and How to Reach the Goal, *International Journal of Smart Grid*, , Vol.3, No.4, pp 188-200,
- [8] N. Chellammal, R. C. Ilambirai, S. SekharDash and K. V. Rahul, "Integration of renewable energy resources in off GRID system using three port zeta converter," *2016 IEEE International Conference on Renewable Energy Research and Applications (ICRERA)*, Birmingham, 2016, pp. 971-976.
- [9] A. Harrouz, I. Colak and K. Kayisli, "Control of a small wind turbine system application," *2016 IEEE International Conference on Renewable Energy Research and Applications (ICRERA)*, Birmingham, 2016, pp. 1128-1133.
- [10] K. D. Mercado, J. Jiménez and M. C. G. Quintero, "Hybrid renewable energy system based on intelligent optimization techniques," *2016 IEEE International Conference on Renewable Energy Research and Applications (ICRERA)*, Birmingham, 2016, pp. 661-666.